

IGF 11 - XI Convegno Nazionale
Gruppo Italiano Frattura
Brescia, 4-6 luglio 1995

**FRACTURE DAMAGE DURING SLIDING WEAR
OF CERAMICS**

**RUOLO DELLA FRATTURA NELL'USURA DI STRISCIAMENTO
DEI CERAMICI**

G. Nicoletto[#], A. Tucci, L. Esposito**

[#] Dip. di Ingegneria Industriale,
Università di Parma
Viale delle Scienze - 43100 Parma

* Centro Ceramico
Via Martelli, 26 - 40138 Bologna

PAROLE CHIAVE. usura, ceramici, frattura

SOMMARIO

Dopo una breve introduzione sul ruolo della frattura sul comportamento ad usura di strisciamento dei materiali ceramici, vengono riportati i risultati sperimentali di una caratterizzazione tribologica di due allumine commerciali con diversa microstruttura. Con una attenta indagine al SEM vengono determinati i principali meccanismi di rimozione del materiale per usura in questi materiali. Sono quindi identificati modelli di meccanica della frattura che possono evidenziare il legame tra microstruttura e resistenza all'usura.

ABSTRACT

After a brief overview of the current understanding of the role of fracture mechanisms during sliding wear testing, selected results on the the friction and wear response of two commercial aluminas with different microstructures are presented along with a SEM investigation of the wear mechanisms involved. Idealized wear damage types and fracture mechanics models are identified with the aim of defining a link between microstructure and wear.

INTRODUCTION

Ceramic materials are increasingly being considered in various extreme tribological applications because of their outstanding mechanical and physical properties, such as strength, hardness, chemical inertness and shock resistance. In the literature relationships are often proposed to describe the dependence of wear on some operating parameters, such as applied load, sliding velocity etc. They have, however, limited applicability at the material selection stage for a given tribological application. Therefore, attempts have been made to develop equations that relate wear response, mechanical properties and wear mechanisms.

This paper begins with a brief overview of the current understanding of the role of fracture mechanisms during sliding wear testing. Selected results of an experimental program aimed at the friction and wear characterization of two commercial aluminas which differ significantly in terms of microstructure are then presented along with a SEM investigation of the wear mechanisms involved. The implication for modelling wear phenomena using fracture mechanics concepts is finally discussed.

ROLE OF FRACTURE IN THE WEAR OF CERAMICS

Three main mechanisms of material deformation and material removal during wear of ceramics have been found, individually and collectively, i) plastic deformation, ii) brittle fracture and iii) tribochemical mechanisms.

i) *Plastic deformation* Although ceramics are brittle in traction, they may show a plastic behavior when the brittle response is inhibited by the hydrostatic pressure associated with concentrated contact forces. This mechanism of deformation should also be favoured by a reduced yield strength due to the frictional heating. The actual material removal mechanism is not clearly defined although fracturing of the plastically deformed but nonetheless brittle material is expected.

ii) *Brittle fracture* The brittle fracture mechanism has been observed and reported by many investigators and are related to the natural brittleness of this class of materials. A test which typifies this behavior is the static indentation test with a Vickers indenter, [1]. In this test two main crack systems develop in the indented material as shown in the top view and cross section of Fig. 1: radial cracks normal to the free surface and lateral cracks which are parallel to the free surface. Several wear models assume that the cracking damage due to indentation is also operative in sliding wear tests and that the material removal occurs due to fragmentation of the material following lateral and radial cracking along the line of sliding. Severe wear in ceramics has been attributed to the brittle fracture mechanism, [2].

iii) *Tribochemical mechanisms* Recent studies, [3], have shown that wear mechanisms in ceramics are not limited to the previous ones but a significant role is played by the tribochemical mechanisms activated through chemical reaction. For example, during sliding contact the heated surface of the material may oxidize thus altering the characteristics of the surface layer. It may result in a change of the friction coefficient and the activation of spalling mechanisms of the oxidized layer.

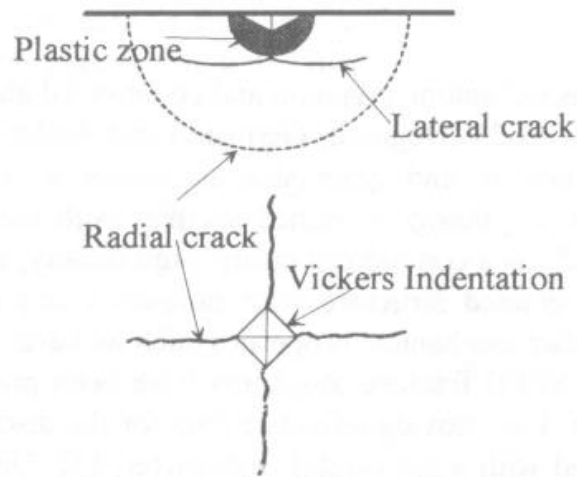


Fig. 1 - Fracture damage during Vickers indentation of ceramics

Various models attempted to correlate basic material properties and wear. Probably the most widely discussed is due to Evans and Marshall, [1]. They assumed that contacting surface asperities and abrasive particles activate Vickers indentation-type fracture mechanisms and derived the following wear rate, W , (volume of material removed, V ,/ distance sled, L ,) equation

$$W=V/L=P^{1.125} K_c^{-0.5} H^{-1.425} E^{0.8} \quad (1)$$

in which P is the contact load, K_c is the fracture toughness and E is the Young's modulus of elasticity. They however found only a qualitative correlation in sliding wear testing of glass and very poor correlation in polycrystalline ceramics.

Of the various bulk material properties of Eq. 1, the fracture toughness is commonly expected to play a fundamental role in the wear performance of ceramics. However, when specifying fracture toughness properties in the context of wear properties, it has become necessary to include aspects related to the microstructural scale of the fracture process. The microstructure of the material, as characterized by density and purity (i.e. presence of a second phase) and average grain size, is expected to largely affect the wear response of ceramics. High density should ensure the absence of macro porosities and other sintering defects while the presence of a second phase would affect the intergranular strength. The role of the grain size is contradictory. Tensile strength and hardness of alumina, one of the most studied ceramic materials for tribological application, often decrease with increasing grain size. Fracture toughness of alumina, [4], increases with increasing grain size because various toughening mechanisms such as grain bridging and crack deflections are activated. Furthermore, wear performance should be affected by surface conditions which are difficult to control and reproduce. Surface cracks generated during mechanical surface finishing favour the activation of surface fracturing.

METHODOLOGY

Two materials were selected among common and commercial aluminas with significantly different microstructure. AL23 (Degussit, Germany) and Alubit (Bitossi, Italy) aluminas have different purity, density and grain size as shown in Tab. 1. Grain size was determined on polished and thermally etched samples with the aid of a computerized image analyzer. The AL23 is a commercial purity, high density, coarse grained structure. The Alubit has a fine grained structure with porosities and abundant second phase (silicate and glassy). Other mechanical properties such as hardness, Vickers indentation fracture toughness and SEPB fracture toughness have been previously determined and are also reported in Tab. 1 to provide reference data for the discussion. A series of wear tests has been performed with a pin-on-disk tribometer, [5]. Disks of AL23 and Alubit were mated with spherically-tipped (2.5 mm radius) pins made of AL23 alumina. The sliding distance in all tests was 3 km under the normal load of 33N. Three sliding velocities, namely 0.3, 0.7 and 1.0 m/s were examined. The friction coefficient was continuously monitored during the test and the material loss measured at the end of each test with a micro balance.

Tab.1 - Physico-mechanical properties of the two aluminas

Property	AL23	Alubit
Density (g/cm ³)	3.91	3.57
Al ₂ O ₃ content (wt. %)	99.6	90.0
Ave. grain size (μm)	7.0	1.8
Hardness HV ₂₀ (GPa)	15.2	9.98
Fracture toughness K _{IC} (MPa m ^{1/2})(*)	5.03	3.17
Fracture toughness K _{IC} (MPa m ^{1/2})(**)	4.20	2.50
Normalized wear rate (Eq. 1)	6.66 10 ⁻⁶	15.73 10 ⁻⁶

(*) Lawn formula; (**) SEPB method

To investigate the role played by the fracture mechanisms during sliding wear after testing the worn disks were examined in the SEM. Besides inspection of the wear tracks for damage mechanism, sectioning normal and tangential to the wear track was performed to investigate the nature and extent of surface and subsurface fracture damage and its dependence on material microstructure and testing conditions.

RESULTS AND DISCUSSION

Friction and wear response

In this section the friction and wear response of the disk materials which undergo cyclic heating and mechanical loadings due to the moving point-wise contact will be presented. The average friction coefficients for the two materials as a function of the sliding velocity are shown in Fig. 2. Friction values are relatively low, less than 0.3 in all cases. The

Alubit shows a limited increase in friction coefficient with sliding velocity, while the AL23 shows an abrupt increase above $v=0.7$ m/s.

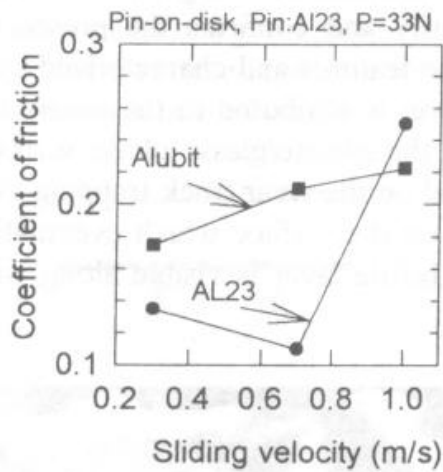


Fig. 2 - Friction coefficients as a function of sliding velocity

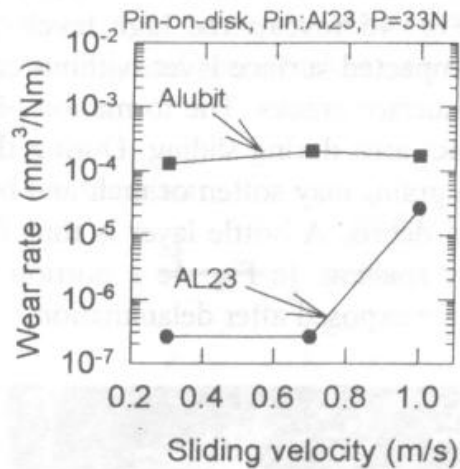


Fig. 3 - Normalized wear rates as a function of sliding velocity

The wear rate dependence on the sliding velocity is shown in Fig. 3. The wear rate data are normalized dividing the volume of material removed by the sliding distance and the nominal applied load. The Alubit shows a wear rate which is independent of the sliding velocity. At low velocity, the AL23 alumina shows a three-orders-of-magnitude lower wear rate than the Alubit. As for the friction coefficient data of Fig. 2, however, the AL23 alumina shows a large (two-order-of magnitude) increase in wear rate above $v=0.7$ m/s. Therefore, the change in friction coefficient and the dramatic increase in wear rate of AL23 could be attributed to a change in the wear mechanisms. This aspect will be discussed in the following section.

Estimates of the wear rate for the two aluminas according to Eq. (1) are given in Tab. 1. For the Alubit, the wear rate is always smaller than the experimental value while in the AL23 the computed value is comparable to the experimental wear rate at high velocity.

Wear mechanisms

The role played by the microstructure is best determined by SEM inspection of the wear tracks. While frontal inspection of wear track is standard, in this work care was devoted to the investigation of the nature and extent of possible subsurface mechanisms. Therefore, careful sectioning normal and tangential to the wear track was performed.

The friction and wear rate dependence on sliding velocity of the AL23 signalled a possible change in wear mechanisms occurring between 0.7 and 1.0 m/s. A smooth surface and fine debris are observed at low velocity. Wear track inspection at the highest velocity, Fig. 4a, also shows smoothed areas following asperity microfracture with the debris generated acting as abrasive particles. However, occasional grain pull out and

flaking is also observed. Fig. 4b shows a radial cross-section of the wear track with evidence of subsurface intergranular cracking which resembles the later cracks of Fig. 1.

The low-purity fine-grained Alubit showed an almost constant wear rate. Fig. 4c shows the wear track where a delaminated layer is easily identified. The tangential cross-section shown in Fig. 4d reveals the high level of porosity and confirms the presence of a strongly compacted surface layer without crystalline features and characterized by many parallel subsurface cracks. The formation of this layer is attributed to the severe heating in the contact area during sliding. During the test, the silicate/glassy phase surrounding the alumina grains may soften or melt and be spread on the wear track trapping the very fine alumina debris. A brittle layer is thus formed on the surface which eventually may come off by spalling. In Fig. 4c a portion of the brittle layer is visible along with the coarse surface exposed after delamination.

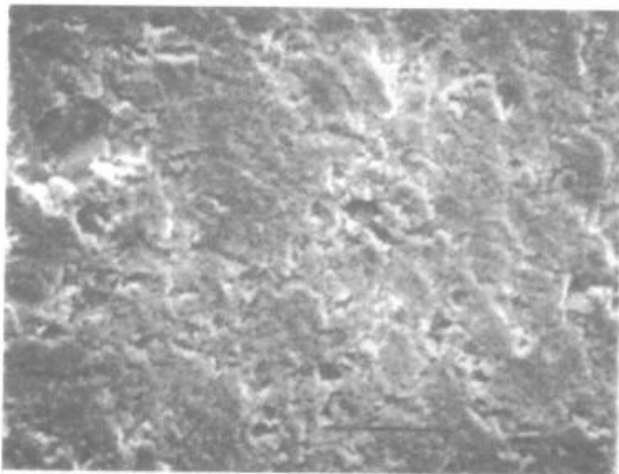


Fig.4 a - Wear track: sliding velocity 1.0 m/s, normal load 33 N, mat: AL23, grain pull-out and flaking is observed

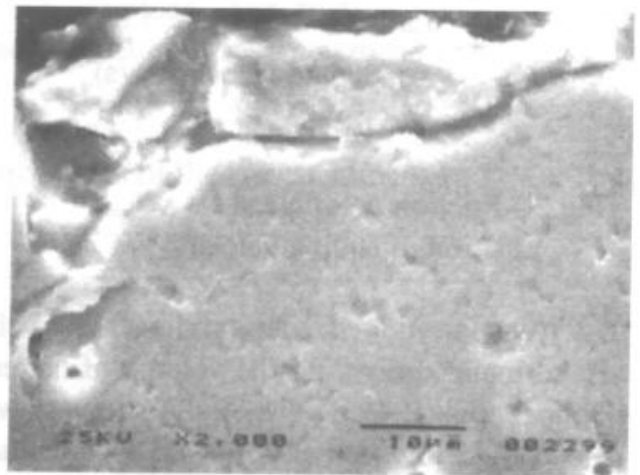


Fig. 4 b - Radial cross-section: sliding velocity 1.0 m/s, normal load 33 N, mat. AL23, subsurface intergranular crack

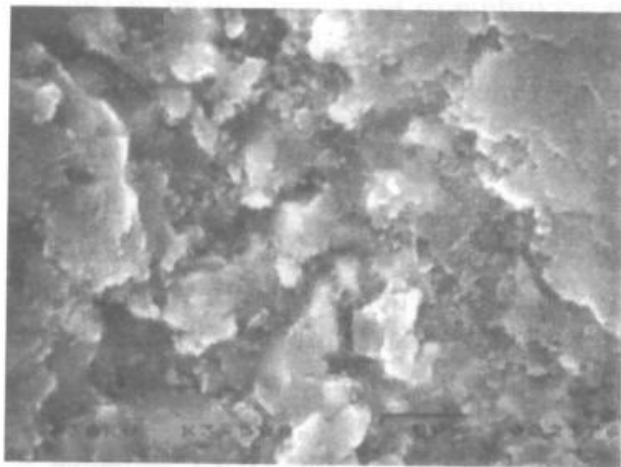


Fig. 4 c - Wear track: sliding velocity 1.0 m/s, normal load 33 N, mat: Alubit

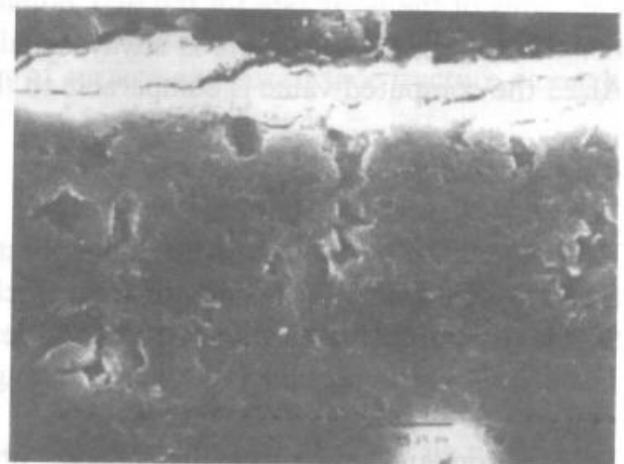


Fig. 4 d - Tangential cross-section sliding velocity 1.0 m/s, normal load 33 N, mat: Alubit, subsurface layer

An attempt to capture the main features of the previous SEM observations is given by the schemes of the damage of Fig. 5. For the AL23, Fig. 5a shows the development of intergranular damage due to contact stresses and heating and Fig. 5b the abraded layer along with occasional grain pull-out. For the Alubit, Fig. 5c depicts the development of a cracked glassy surface layer due to localized heating and second phase melting and Fig. 5d the spallation of the layer.

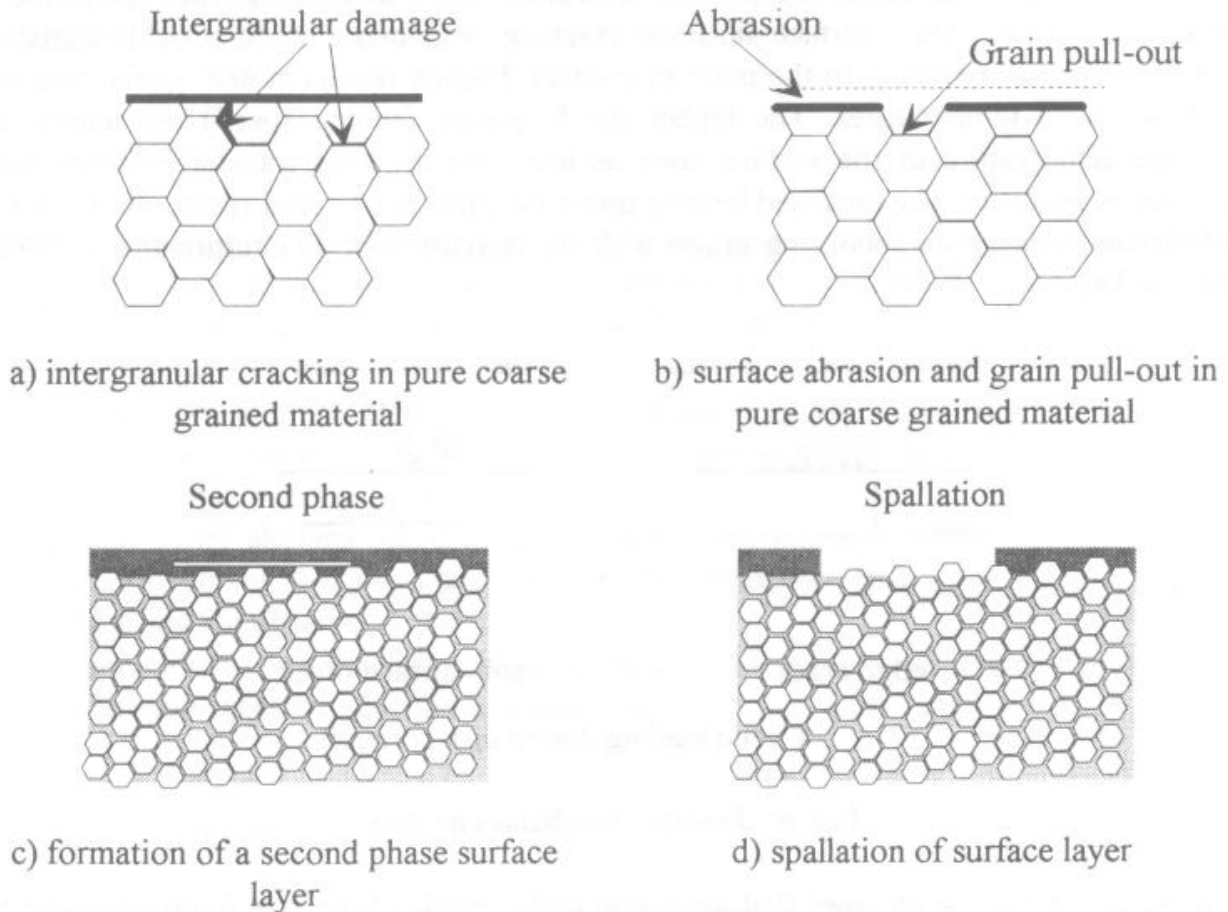


Fig.5 - Idealized damage models based on SEM observations

Implication for modeling

Wear is perhaps the most complex phenomenon to be examined by fracture mechanics, [6]. The analysis is complicated by rapidly varying complex stress systems, environmental effects, large plastic strains, crack sizes on the order of the microstructural dimensions. The previous section revealed how the sliding load resulted in cracking and/or material removal. In order to properly model the previous wear mechanisms the causes of damage has to be discussed in the first place and the criteria for damage evolution should then be identified.

A sliding contact results in severe stress fields. The elastic stress field for a sliding circular contact on a flat plane has been obtained in [7] by superposition of static normal stresses and the tangential load stresses. The stress state in the disk material include a

nearly hydrostatic compression. The main difference with the classical Hertz solution is the development of a tensile peak stress parallel to the free surface of a trailing edge of the contact. The maximum tensile stress is given by:

$$\sigma_x = \frac{3P}{2\pi a} \left[\frac{1-2\nu}{3} + \frac{4-\nu}{8} \pi f \right] \quad (2)$$

where P is the normal load, a is the contact radius, ν is the Poisson's ratio and f is the friction coefficient. Its effect is especially critical for brittle materials as they are prone to failure in tension. Also, surface finishing cracking or damage could provide initiation sites for material removal. In the point of contact, friction results in heat generation and high localized temperatures. The higher the frequency (sliding speed) the higher the average temperature of the surface layer as less time for heat transfer between each passage is available. The localized heating under the point load could result in differential dilatations between neighbouring grains with the development of intergranular damage, Fig. 5a, [8].

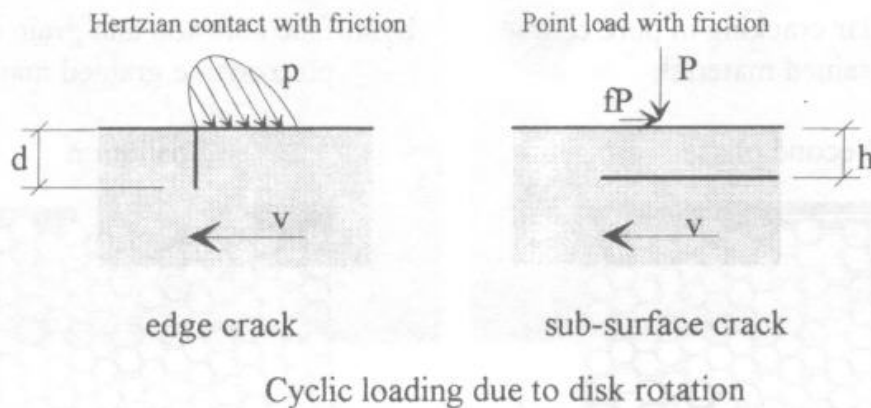


Fig. 6 - Fracture mechanics models

The model of Fig. 6a assumes that an intergranular crack whose size is proportional to the average grain size, d , may develop due to one of the previous mechanisms and will propagate (grain unlocking) due to the travelling contact load. Therefore

$$K \propto \sigma_x(d)^{1/2} = K_c \quad (3)$$

where K_c is the intergranular toughness of the material. The geometry factor is neglected for simplicity. This relation shows that a reduction in grain size and friction coefficient would improve the wear performance.

For a low purity material the previous SEM investigation showed the development of a surface layer with subsurface cracks. The model of Fig. 6b defines the key parameters controlling the growth of a subsurface crack which are primarily caused by the action of shear stresses and hindered by interference between the opposing crack faces. It involves fracture under mixed mode loading and the solution for a sliding point load gives a general idea of the problem, [9],

$$K_{II} \propto f P(h)^{-1/2} = K_{IIC} \quad (4)$$

For a relatively long crack and for a given load, the thickness of the brittle layer becomes a critical dimension and it may depend on the percentage of the second phase. K_{IIC} is the toughness in shear of the second phase which should be quite lower than for an alumina.

These two crack models related to wear mechanisms attempt to capture the basic features associated to the interaction of the complex tensile stresses due to the sliding pin and the non-homogenous material microstructure. They do not provide, however, an estimate of the wear rate: work on this aspect is in progress.

CONCLUSIONS

The friction and wear characterization of two commercial aluminas which differ significantly in terms of microstructure have been presented along with a detailed SEM investigation of the wear mechanisms. Pin-on-disk tests showed a different response of the two materials:

- the low-purity alumina presented almost constant friction coefficients and wear rates with increasing sliding velocity. Formation of a brittle surface layer which is subjected to spalling was found at all velocities;
- the high-purity alumina presented a remarkable increment in friction coefficient and wear rate above 0.7 m/s. Only above that velocity, grain pull-out and flaking mechanisms are observed;
- two simple models addressing the interaction of the complex sliding contact stresses and the material microstructure are identified.

ACKNOWLEDGEMENTS

G. N. acknowledges with thanks partial support of this research by Ministero dell'Università e della Ricerca Scientifica e Tecnologica

REFERENCES

- [1]. A.G. Evans, D.B. Marshall, Fundamental of friction and wear, D.A. Rigney Ed., ASM, Metals Park, 1981, p.439
- [2]. O.O. Ajayi, K.C. Ludema, "Surface damage of structural ceramics: implications for wear modeling", *Wear*, Vol. 124,1988, pp. 237-257
- [3]. T.E. Fisher, H. Tomizawa, "Interaction of tribochemistry and microfracture in the friction and wear of silicon nitride", *Wear*, Vol. 105, 1985, pp. 29-45
- [4]. G. Nicoletto, L. Esposito, "The effect of microstructure on the fracture toughness of polycrystalline alumina", *Fatigue and Fracture of Engineering Materials and Structures*, Vol.19, 1, 1996, pp.119-128

- [10] Bažant, Z.P., Pfeiffer, P.A., 'Determination of fracture energy from size effect and brittleness number', *ACI Material Journal*, November-December, 463-480, 1987.
- [11] Schlangen, E., 'Experimental and numerical analysis of fracture process in concrete', *Heron*, 38, 1993.
- [12] Barr, B., Tokatly, Z.Y., 'Size effects in two compact test specimen geometries', *Applications of Fracture Mechanics to Reinforced Concrete*, (Ed. A. Carpinteri), Elsevier Applied Science, London, 63-93, 1991.
- [13] Tokatly, Z.Y., Barr, B., 'Size effects in mode III fracture', *Fracture Processes in Concrete, Rock and Ceramics*, (Eds. J.G.M. van Mier and A. Bakker), E.& F.N. Spon, 473-482, 1991.